Journal of Materials Chemistry C

Aggregation-Induced Emission, Mechanochromism and Blue Electroluminescence of Carbazole and Triphenylamine-Substituted Ethenes

Journal:	*Journal of Materials Chemistry C*
Manuscript ID:	TC-ART-01-2014-000097.R1
Article Type:	Paper
Date Submitted by the Author:	28-Feb-2014

Complete List of Authors:	Chan, Carrie; The Hong Kong University of Science and Technology, Department of Chemistry Lam, Jacky Wing Yip; The Hong Kong University of Science and Technology, Department of Chemistry Zhao, Zujin; South China University of Technology, State Key Laboratory of Luminescent Materials and Devices Chen, Shuming; The Hong Kong University of Science and Technology, Department of Electronic and Computer Engineering Lu, Ping; Jilin University, Key Laboratory for Supramolecular Structure and Materials of Education of Ministry Sung, Herman; The Hong Kong University of Science and Technology, Department of Chemistry Kwok, Hoi; The Hong Kong University of Science and Technology, Department of Electronic and Computer Engineering Ma, Yuguang; Jilin University, Key Laboratory for Supramolecular Structure and Materials of Education of Ministry Williams, Ian; The Hong Kong University of Science and Technology, Department of Chemistry Tang, Ben Zhong; The Hong Kong University of Science and Technology, Department of Chemistry

SCHOLARONE™
Manuscripts

Journal Name

RSCPublishing

ARTICLE

Aggregation-Induced Emission, Mechanochromism and Blue Electroluminescence of Carbazole and Triphenylamine-Substituted Ethenes

Cite this: DOI: 10.1039/xoxxoooooox

Received ooth January 2012,
Accepted ooth January 2012

DOI: 10.1039/xoxxoooooox

www.rsc.org/

Carrie Y. K. Chan,[a] Jacky W. Y. Lam,[a] Zujin Zhao,[b] Shuming Chen,[c] Ping Lu,[d] Herman H. Y. Sung,[a] Hoi Sing Kwok,[c] Yuguang Ma,[d] Ian D. Williams,[a] and Ben Zhong Tang[a,b,e,f,*]

Carbazole and triphenylamine-substituted ethenes are synthesized [Ph_2C=CPh(R) R= 9-carbazolyl, 9-hexyl-3-carbazolyl and 4-(diphenylamino)phenyl] and their optical properties are investigated. All the luminogens are nonemissive when molecularly dissolved in good solvents but become highly emissive in the aggregated state, showing a phenomenon of aggregation-induced emission. High solid-state fluorescence quantum yields up to 97.6% have been achieved in their solid thin films. The luminogens are thermally stable, showing high degradation temperatures of up to 315 ^{o}C. They exhibit mechanochromism: their emissions can be repeatedly switched between blue and green colors by simple grinding-fuming and grinding-heating processes due to the morphological change from crystalline to amorphous state and vice versa. Multilayer light-emitting diodes with device configurations of ITO/NPB/dye/TPBi/Alq_3/LiF/Al, ITO/NPB/dye/TPBi/LiF/Al and ITO/dye/TPBi/LiF/Al are fabricated, which emit sky blue lights with maximum luminance, current efficiency, power efficiency and external quantum efficiency of 11700 cd/m^2, 7.5 cd/A, 7.9 lm/W and 3.3%, respectively.

Introduction

Since Tang demonstrated the use of organic light emitting diodes (OLEDs) with multilayer structures to improve the device performances, a large number and a wide variety of organic fluorophores have been prepared.[1] In OLEDs, the emitters are fabricated as thin films and their device performances depend somewhat on their solid-state fluorescence quantum yields ($\Phi_{F,F}$). However, many organic fluorophores are nonluminescent or weakly emissive in the solid state, although their dilute solutions emit strongly under UV irradiation. This is attributed to the strong intermolecular electronic interactions in the solid state, which favour the formation of detrimental species such as excimers and exciplexes. Such phenomenon is coined as "aggregation-caused quenching" (ACQ) and has been a textbook-knowledge.[2] In contrast to a large number of ACQ molecules, examples of highly emissive organic solids with high $\Phi_{F,F}$ values are still rare, especially those with strong solid-state blue emission. It is therefore challenging to achieve stable and efficient solid-state blue emitters compared with green and red emitters as the performances of current blue OLEDs are still much beyond than those of the green and red ones. With the fact that blue is one of the primary colors, it is essential for the fabrication of full-color displays. In addition, blue-emitting materials may act as host materials for green and red dopants.

Recently, we and other groups observed that a novel phenomenon of aggregation-induced emission (AIE) which is exactly opposite to the ACQ effect: a series of propeller-like molecules are practically nonluminescent when molecularly dissolved in good solvents but become highly emissive when aggregated into nanoparticles in poor solvents or fabricated as thin films in the solid state.[3,4] The AIE effect enables the molecules to find high-tech applications as chemical sensors, biological probes, stimuli-responsive nanomaterials and active layers for the fabrication of OLEDs.[5] Among the AIE luminogens, tetraphenylethene (TPE) possesses a simple molecular structure with a splendid AIE effect (Chart 1). However, its EL performance is quite poor with maximum luminance (L_{max}), current efficiency ($\eta_{C,max}$) and external quantum efficiency ($\eta_{ext,max}$) of 1800 cd/m^2, 0.45 cd/A and 0.4%, respectively.[6] Carbazole and triphenylamine (TPA) are well-known hole-transporting materials but suffer from ACQ effect in the condensed state. Incorporation of TPE into their structures has solved their ACQ problem and meanwhile generates efficient solid-state emitters such as TPECa and TPATPE with unity $\Phi_{F,F}$ values. OLEDs fabricated using TPECa and TPATPE show good device performances. For example, the EL device of TPECa with a configuration of ITO/NPB/TPECa/TPBi/Alq_3/LiF/Al exhibits a L_{max} of 7508 cd/m^2 and $\eta_{ext,max}$ of 1.8%.[7] The performance of EL device based on TPATPE is more impressive, exhibiting L_{max} and

$\eta_{ext,max}$ of 26090 cd/m^2 and 3.3%, respectively.[8] Both TPECa and TPATPE can play dual roles as light-emitting and hole-transporting layers in OLED. This simplifies the device structure and helps reduce the fabrication cost.

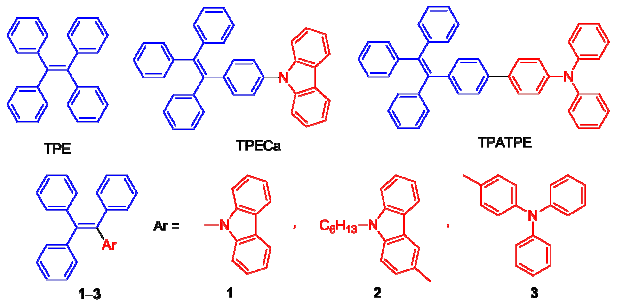

Chart 1. Molecular structures of tetraphenylethene and its derivatives containing carbazole and triphenylamine units.

Mechanochromic luminescent materials, which show emission color or intensity change induced by mechanical stress, have aroused increasing interest in recent years due to their potential applications in many fields such as sensors, displays and memories.[9] Taking their advantage of high $\Phi_{F,F}$ values, AIE-active molecules are thus considered as promising candidates for such applications. A variety of AIE luminogens with various functionalities have been prepared. However, AIE molecules with mechanochromic fluorescence properties are seldom reported. With such regard, we designed and synthesized new luminogens from triphenylethene, carbazole and TPA building blocks (**1**–**3**; Chart 1). Unlike TPECa and TPATPE, the carbazole and TPA units serve as skeletons, rather than substituents, for the construction of **1**–**3**. Luminogens **1**–**3** exhibit not only AIE characteristics but also intriguing mechanochromism due to the morphological change from the crystalline to amorphous state and vice versa. Multilayer OLEDs utilizing the new luminogens are fabricated, which show blue light in high luminance and current efficiency up to 11700 cd/m^2 and 7.5 cd/A, respectively.

Results and discussion

Synthesis

To enrich the AIE research and widen their practical applications, we designed the molecular structures of three new AIE luminogens and elaborated a multistep reaction route for their syntheses (Scheme 1). Compound **5** was first prepared by reaction of carbazole (**4**) with benzyl bromide in the presence of tetrabutylammonium bromide under basic condition. Lithiation of **5** followed by reaction with benzophenone and acid-catalyzed dehydration afforded **1**. On the other hand, the Friedel-Crafts acylation of benzoyl chloride (**7**) with 9-hexyl-

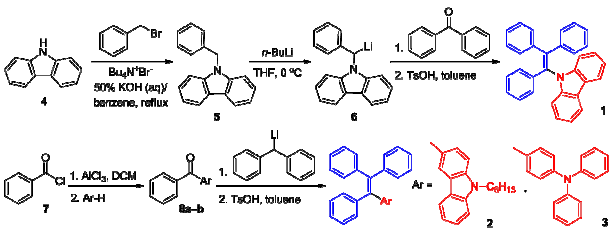

Scheme 1. Synthetic routes to carbazole and triphenylamine-substituted ethenes.

carbazole and TPA furnished **8a** and **8b**, which converted into **2** and **3**, respectively, by their reaction with diphenylmethyllithium followed by acid-catalyzed dehydration. All the intermediates and final products were carefully purified and fully characterized by NMR and mass spectroscopies, from which satisfactory analysis data corresponding to their expected molecular structures were obtained. Single crystals of **1**–**3** were grown from their dichloromethane/methanol solutions and characterized crystallographically. Their ORTPE drawings are shown in Figure 1 and the associated crystal data are summarized in Table S1 in the Supporting Information. All the luminogens are soluble in common organic solvents, such as tetrahydrofuran, toluene, dichloromethane and chloroform, but insoluble in water.

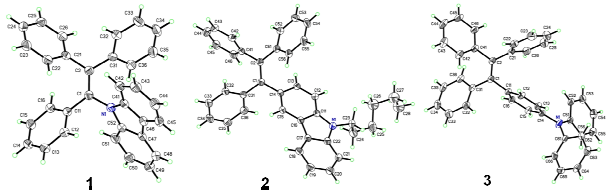

Figure 1. ORTEP drawings of **1**–**3** (CCDC 970451–970453).

Optical properties

The dilute THF solution (10 μM) of **1** exhibits a peak maximum at 341 nm. The spectra of **2** and **3**, however, are located at longer wavelength, revealing that they possess a better conjugation. Like other AIE luminogens prepared previously, the photoluminescence (PL) spectra of **1**–**3** in dilute THF solutions (10 μM) exhibit only noisy PL signals with no discernible peak maxima (Figure 3, S1 and S2). The solution-state fluorescence quantum yields ($\Phi_{F,S}$) of **1** and **2** estimated using 9,10-diphenylanthracene as standard are merely 0.70% and 0.27% respectively, indicating that they are weak emitters when molecularly dissolved in good solvents. These values are much lower than those of carbazole (37%)[10a] and TPA (13.0),[10b] suggesting that the triphenylvinyl unit in **1**–**3** works as a PL quencher in the solution state.

This journal is © The Royal Society of Chemistry 2012

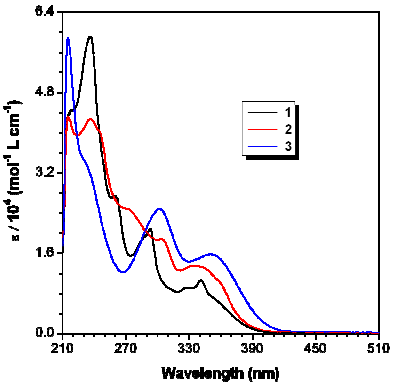

Figure 2. UV spectra of **1**–**3** in THF solutions. Solution concentration: 10^{-5} M.

Whereas luminogens **1**–**3** are almost non-fluorescent in solutions, they emit intensely in the aggregated state. As shown in Figure 3, the PL intensity of **1** remains low in aqueous mixtures with less than 80% water content but starts to increase swiftly afterwards. The emission intensity reaches its maximum at 95% water fraction. From the pure THF solution to THF/H_2O mixture with 90% water content, the PL intensity rises by 350-fold. Similar phenomena are also observed in **2** and **3** (Figure S1 and S2). Clearly, the emissions of **1**–**3** are induced by aggregate formation, or in other words, they are AIE-active. In dilute solution, the rotation of the multiple phenyl rings has consumed the energy of the excitons through nonradiative relaxation channel and thus has quenched the light emission of the dye molecules. In the aggregate state, the intramolecular rotation (IMR) is restricted, thus allowing the luminogens to emit intensely. We further investigated the PL behaviors of the **1**–**3** in the solid state. The emissions of their thin films are observed at 465–500 nm, which are similar to the PL of their aggregates in THF/H_2O mixtures (Table 1). The $\Phi_{F,F}$ value of **3** (97.6%) measured using a calibrated integrating sphere is much higher than those of **1** and **2** (55.7% for **1** and 33.1% for **2**), presumably due to its higher conjugation.

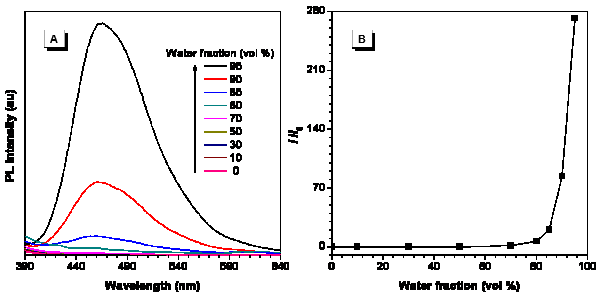

Figure 3. (A) PL spectra of **1** in THF and THF/H_2O mixtures with different water fractions. Concentration: 10^{-5} M; excitation wavelength: 340 nm. (B) Plot of I/I_0 values versus the compositions of the THF/H_2O mixtures of **1**.

Table 1. Absorption and emission of **1**–**3** in the solution (Soln)[a], aggregated (Aggr)[b], crystalline (Cryst) and amorphous (Amor)[c] states.

Luminogen	λ_{ab} (nm)[d]	λ_{em} (nm)[e]			
	Soln	Soln ($\Phi_{F,S}$)	Aggr	Cryst	Amor ($\Phi_{F,F}$)
1	341	(0.70)	466	455	465 (55.7)
2	342	(0.27)	489	454	490 (33.1)
3	350	(1.22)	499	429	500 (97.6)

[a]In dilute THF solution (10 μM). [b]In THF/H_2O mixture (1:9 by volume). [c]In solid thin film. [d]Absorption maximum. [e]Emission maximum with quantum yield (%) given in the parentheses. $\Phi_{F,S}$ = Fluorescence quantum yield in THF solution determined using 9,10-diphenylanthracene (Φ_F = 90% in cyclohexane) as standard. $\Phi_{F,F}$ = fluorescence quantum yield for thin film measured by a calibrated integrating sphere.

To gain a deep insight into the optical behaviors of the luminogens, we performed theoretical calculations on their energy levels. Their highest occupied (HOMO) and lowest unoccupied (LUMO) molecular orbitals plots are given in Figure 4. The triphenylvinyl units are twisted from the plane of the carbazole or TPA unit in all the molecules, which prevent emission quenching caused by unfavourable π–π stacking interaction. Whereas the HOMO of **1** and **2** are dominated by the orbitals from the carbazole ring and part of the triphenylvinyl unit, the orbitals of their LUMO are located mainly on the latter one. On the other hand, the electron cloud of the HOMO of **3** is located mainly on the TPA unit. However, it shows almost no contribution to the LUMO energy level. The calculated band gaps for **1**–**3** are 3.80, 3.85 and 3.61 eV, respectively.

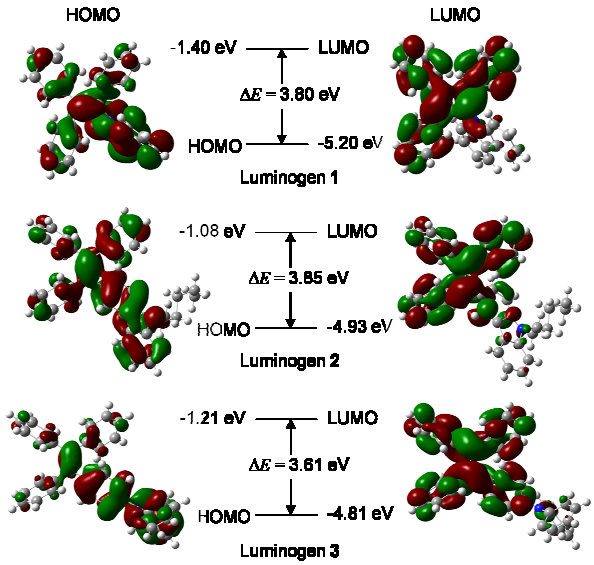

Figure 4. Molecular orbital amplitude plots of HOMO and LUMO levels of **1**–**3** calculated using the B3LYP/6-31G* basis set.

Interestingly, the crystals of **1**–**3** emit at 429–455 nm, which are 10–71 nm blue-shifted from those of the amorphous films. The unusual blue shift observed in the crystalline phase may be attributable to the conformation twisting of the aromatic rings of the luminogens in order to fit into the crystalline lattices. Without such restraint, the molecules in the amorphous state may assume a more planar conformation and thus show a redder luminescence. To gain further insight into the AIE mechanism, we checked the geometric structures and packing arrangements of **1** and **3** in the crystalline state. As shown in Figure 5, multiple C–H···π hydrogen bonds with distances of 2.620 and 3.075 Å are formed between the carbazolyl protons of one molecule of **1** and the π cloud of carbazole unit of neighbouring molecule. Similar interactions are also observed in **3**. These multiple C–H···π hydrogen bonds help rigidify the molecular conformation and have locked the molecular rotation. As a result, the excited state energy consumed by the IMR process is greatly reduced, thus enabling **1** and **3** to emit intensely in the solid state. The dihedral angles between the vinyl core and the carbazole or triphenylamine unit are 43.7°, 46.1° and 53.0° for **1**–**3**, respectively. This suggests that **3** takes a more twisted conformation, thus leading to bluer crystal emission and the largest hypochromic PL shift from aggregated to crystal state.

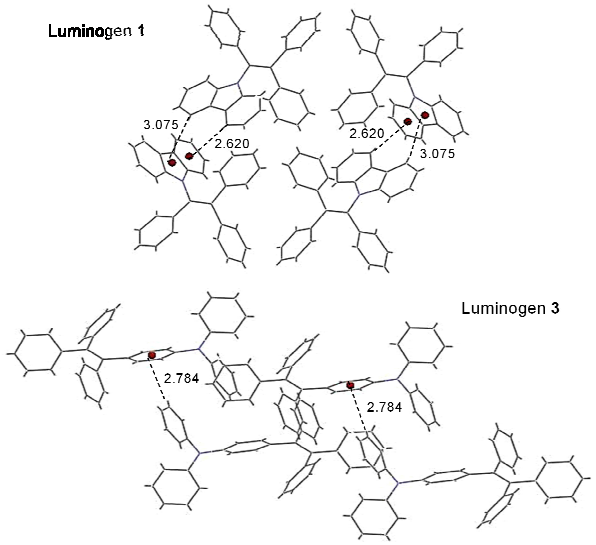

Figure 5. Perspective view of the packing arrangements in crystals of **1** and **3**. The aromatic C–H···π hydrogen bonds are denoted by dotted lines.

Upon gentle grinding the crystals of **3** using a spatula or pestle, their emission changes from blue to green (Figure 6), demonstrating a property of mechanochromic fluorescence. Since the PL of the mechanically agitated crystals is close to that of the amorphous film (Figure 7A), such phenomenon should be associated with the morphological change from crystalline to amorphous state. This is supported by the result from powder X-ray diffraction analysis: whereas the diffractogram of the crystals exhibit many sharp peaks, that of the mashed crystals show fewer and broader peaks with much weaker intensities, indicating that they, in a large extent, are amorphous nature (Figure S3). After solvent fuming to acetone vapour at room temperature for 10 min or heating at 120 °C in

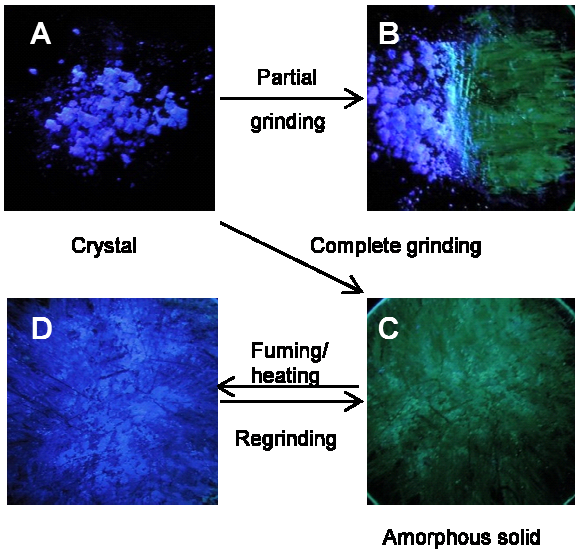

Figure 6. Reversibly switching between the blue crystalline and green amorphous states of **3** by grinding-fuming and grinding-heating cycles. The photographs were taken under 365 nm UV irradiation from a hand-held UV lamp.

air for 10 min, the green powders recrystallize and are restored nearly to the blue form. The switching between the blue crystalline and green amorphous states of **3** can be repeated for many cycles without fatigue because these processes are nondestructive in nature (Figure 7B). We believe that by applying a larger pressure load using a hydraulic presser, a more drastic fluorescence shift will be observed. The change in reflectivity has been commonly used as an output in rewritable optical media. A luminescence-based process is of advantage because it offers higher sensitivity, lower background noise and potential for two-dimensional imaging.[11] Luminogen **3** is thus a promising candidate for innovative applications in optical information storage systems.

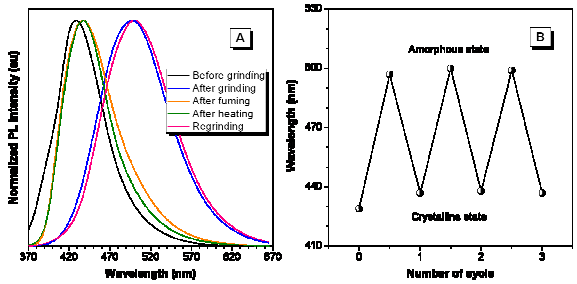

Figure 7. (A) Change in the PL spectrum of crystals of **3** by grinding-fuming and grinding-heating processes. (B) Repeated switching the light emission of **3** by grinding-fuming cycle.

This journal is © The Royal Society of Chemistry 2012

Thermal properties

The thermal stability of **1**–**3** was evaluated by thermogravimetric analysis (TGA) under nitrogen at a heating rate of 10 °C/min. As shown in Figure 8, all the luminogens are thermally stable, losing 5% of their weights at temperatures (T_d) from 294 to 315 °C. Their thermal transitions were investigated by differential scanning calorimetry (DSC) at a heating rate of 10 °C/min. All the compounds exhibit clear melting transitions (T_m) in the range of 174–207 °C. They also possess good morphological stability, as suggested by their reasonably high glass-transition temperatures (T_g) of 72, 50 and 66 °C, respectively. Coupled with their efficient solid-state emission, luminogens **1**–**3** are thus promising EL materials.

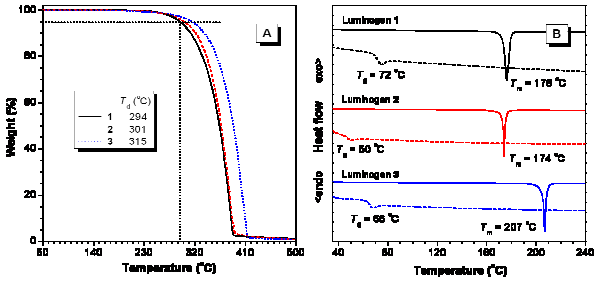

Figure 8. (A) TGA curves and (B) DSC thermograms of first (solid lines) and second (dotted lines) heating scans of **1**–**3** recorded under nitrogen at a heating rate of 10 °C/min.

Electroluminescence

The efficient light emission and high thermal stability of **1**–**3** encourage us to investigate their electroluminescence (EL) properties. Multilayer OLEDs with configurations of ITO/NPB (50 nm)/LEL (20 nm)/TPBi (30 nm)/Alq_3 (20 nm)/LiF (1 nm)/Al (100 nm) (Device I) and ITO/NPB (50 nm)/LEL (20 nm)/TPBi (30 nm) /LiF (1 nm)/Al (100 nm) (Device II) were constructed, where luminogens **1**–**3** worked as light-emitting layer (LEL), NPB functioned as hole-transporting material, TPBi served as electron-transporting and/or hole-blocking layer and Alq_3 worked as electron-transporting material, respectively. The performances and EL data are depicted and summarized in Figure 9 and Table 2. Devices I of **1**–**3** emit bright sky blue EL at 468–488 nm, which are close to the PL spectra of their amorphous thin films. This indicates that both EL and PL originate from the same radiative decay of the singlet excitons. Among the luminogens, OLED based on **3** shows the best performance. The device is turned on at a low voltage of 3.2 V and exhibits a L_{max} of 7140 cd/m^2. The $\eta_{C,max}$, maximum power efficiency ($\eta_{P,max}$) and $\eta_{ext,max}$ attained by the device are 7.5 cd/A, 7.9 lm/W and 3.3%, respectively. Compare to previous results obtained from other AIE luminogens, these values are pretty high. Removal of the Alq_3 layer in Device I forms Device II, which results in different consequences. Whereas the EL performance of Device II of **1** is slightly better than that of Device I, those of **2** and **3** become poorer though the EL devices exhibit higher L_{max} value.

Materials with multi-functional properties, such as light-emitting and hole- and/or electron-transporting capabilities, are more useful for technological applications and in great demand because it can greatly simplify the device structure and reduce the fabrication cost. Carbazole and TPA are well-known for their light-emitting and hole-transporting properties. Since luminogens **1**–**3** are constructed from these moieties, they may serve as bifunctional materials. To test such possibility, OLEDs with a configuration of ITO/LEL/TPBi (40 nm)/LiF (1 nm)/Al (100 nm) are constructed, where **1**–**3** served as both light-emitting and hole-transporting layers. Again, luminogen **3** shows the best EL performance. Its EL device emits at 488 nm, showing L_{max}, $\eta_{C,max}$, $\eta_{P,max}$ and $\eta_{ext,max}$ of 11700 cd/m^2, 2.4 cd/A, 1.0 lm/W and 1.1%, respectively (Figure 10). These values, however, are much inferior than those of Device I and II, leaving much room for further improvement. Nevertheless, the EL data given in Table 2 demonstrate the great potential of the present luminogens as solid light-emitters for the construction of efficient EL devices.

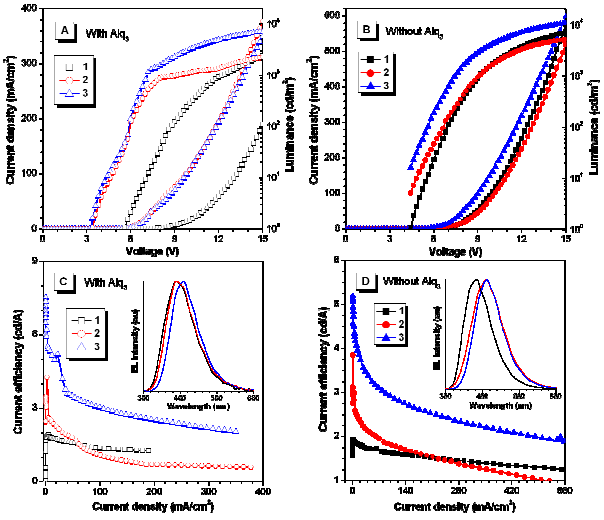

Figure 9. Plots of (A and B) current density and luminance versus voltage and (C and D) current efficiency versus current density in multilayer light-emitting diode of **1**–**3** with device configurations of (A and C) ITO/NPB/LEL/TPBi/Alq_3/LiF/Al and (B and D) ITO/NPB/LEL/TPBi/LiF/Al. Inset in (C) and (D): EL spectra of **1**–**3**.

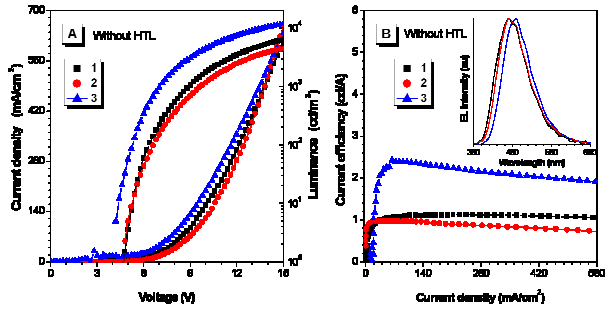

Figure 10. Plots of (A) current density and luminance versus voltage and (B) current efficiency versus current density in multilayer light-emitting diode of **1**–**3** with a device configuration of ITO/LEL/TPBi/LiF/Al. Inset in (B): EL spectra of **1**–**3**.

Table 2. EL Performances of **1**–**3**[a]

Dye	λ_{EL} (nm)	V_{on} (V)	L_{max} (cd/m^2)	$\eta_{P,max}$ (lm/W)	$\eta_{C,max}$ (cd/A)	$\eta_{ext,max}$ (%)
Device I: ITO/NPB/LEL/TPBi/Alq_3/LiF/Al						
1	468	5.6	2410	0.8	1.9	1.0
2	468	3.4	2240	3.2	4.3	1.8
3	488	3.2	7140	7.9	7.5	3.3
Device II: ITO/NPB/LEL/TPBi/LiF/Al						
1	472	4.4	7160	1.2	1.9	1.3
2	492	4.4	5130	2.0	3.9	1.7
3	492	4.0	10900	3.7	5.2	3.1
Device III: ITO/ LEL/TPBi/ LiF/Al						
1	488	4.0	6300	0.4	1.1	0.6
2	492	4.6	4390	0.5	1.0	0.4
3	488	1.0	11700	1.0	2.5	1.1

[a]Abbreviation: LEL = light-emitting layer, λ_{EL} = electroluminescence maximum, V_{on} = turn-on voltage at 1 cd/m^2, L_{max} = maximum luminance, $\eta_{P,max}$ = maximum power efficiency, $\eta_{C,max}$ = maximum current efficiency and $\eta_{ext,max}$ = maximum external quantum efficiency.

Conclusions

In this work, we designed and synthesized a group of carbazole and triphenylamine-substituted ethenes (**1**–**3**). All the luminogens are well characterized by spectroscopic techniques and their chemical structures are further confirmed by X-ray crystallography. Whereas they are nonemissive in dilute THF solutions, they become strong emitters when aggregated in poor solvents or fabricated as films in the solid state, demonstrating a phenomenon of AIE. These luminogens exhibit high solid-state fluorescence quantum yields of up to 97.6% and enjoy high thermal stability (T_d up to 315 ^oC). They also show intriguing mechanochromic fluorescence properties: their emission can be repeatedly switched between blue and green colors by simple grinding-fuming and grinding-heating processes due to the morphological change from crystalline to amorphous state and vice versa. OLEDs using **1**–**3** as emitters are fabricated, which show high luminance and current and external quantum efficiencies of up to 11700 cd/m^2, 7.5 cd/A and 3.3 %, respectively.

Experimental Section

Materials and instrumentations

Dichloromethane (DCM) and tetrahydrofuran (THF) were distilled from calcium hydride and sodium benzophenone ketyl, respectively, under nitrogen immediately prior to use. All the chemicals and other reagents were purchased from Aldrich and used as received without further purification. ^1H and ^{13}C NMR spectra were measured on a Bruker AV 300 spectrometer in deuterated chloroform using tetramethylsilane (TMS; $\delta = 0$) as internal reference. High resolution mass spectra (HRMS) were recorded on a GCT premier CAB048 mass spectrometer operating in MALDI-TOF mode. UV spectra were measured on a Milton Roy Spectronic 3000 Array spectrophotometer. Photoluminescence (PL) was recorded on a Perkin-Elmer LS 55 spectrofluorometer. Thermogravimetric analysis (TGA) was carried on a TA TGA Q5000 under nitrogen at a heating rate of 10 ^oC/min. The thermal transitions of the luminogens were investigated by differential scanning calorimetry (DSC) using a TA DSC Q1000 under dry nitrogen at a heating rate of 10 ^oC/min. Single crystal X-ray diffraction intensity data were collected at 100 K on a Bruker–Nonices Smart Apex CCD diffractometer with graphite monochromated Mo Kα radiation. Processing of the intensity data was carried out using the SAINT and SADABS routines and the structure and refinement were conducted using the SHELTL suite of X-ray programs (version 6.10). The ground-state geometries were optimized using the density functional (DFT) with B3LYP hybrid functional at the basis set level of 6-31G*. All the calculations were performed using Gaussian 03 package.

Device fabrication

The devices were fabricated on 80 nm-ITO coated glasses with a sheet resistance of 25Ω/□. Prior to load into the pretreatment chamber, the ITO-coated glasses were soaked in ultrasonic detergent for 30 min, followed by spraying with de-ionized water for 10 min, soaking in ultrasonic de-ionized water for 30 min and oven-baking for 1 h. The cleaned samples were treated by perfluoromethane plasma with a power of 100 W, gas flow of 50 sccm and pressure of 0.2 Torr for 10 s in the pretreatment chamber. The samples were transferred to the organic chamber with a base pressure of 7×10^{-7} Torr for the deposition of *N*,*N*-bis(1-naphthyl)-*N*,*N*-diphenylbenzidine (NPB), emitter, 2,2',2"-(1,3,5-benzinetriyl)tris(1-phenyl-1-H-benzimidazole) (TPBi) and/or tris(8-hydroxyquinolinato)aluminium (Alq_3) which served as hole-transporting, light-emitting and hole-blocking and electron-transporting layers, respectively. The samples were then transferred to the metal chamber for cathode deposition which composed of lithium fluoride (LiF) capped with aluminium (Al). The light-emitting area was 4 mm^2. The current density-voltage characteristics of the devices were measured on a HP4145B semiconductor parameter analyzer. The forward direction photons emitted from the devices were detected by a calibrated UDT PIN-25D silicon photodiode. The luminance and external quantum efficiencies of the devices were inferred from the photocurrent of the photodiode. The EL spectra were obtained by a PR650 spectrophotometer. All the measurements were carried out under air at room temperature without device encapsulation.

Preparation of nanoaggregates

Stock THF solutions of the compounds with a concentration of 10^{-3} M were prepared. Aliquots of the stock solution were transferred to 10 mL volumetric flasks. After appropriate amounts of THF were added, water was added dropwise under vigorous stirring to furnish 10^{-5} M solutions with different water contents (0–95 vol %). The PL measurements of the resulting solutions were then performed immediately.

Synthesis

Synthesis of 9-benzylcarbazole (5). Into a 100 mL one-necked round bottom flask were added carbazole (**4**, 3 g, 17.9 mmol), benzyl bromide (2.56 g, 15.0 mmol), tetrabutylammonium bromide (0.48 g, 0.15 mmol), 50 wt% of aqueous KOH solution (30 mL) and benzene (30 mL). The reaction mixture was heated to reflux overnight. After cooled to room temperature, the reaction mixture was extracted with DCM. The organic layer was washed with water and dried over magnesium sulfate. After filtration and solvent evaporation, the crude product was purified by silica-gel column chromatography using hexane as eluent. White solid of **5** was obtained in 88.1% yield

This journal is © The Royal Society of Chemistry 2012

(3.39 g). ^{1}H NMR (300 MHz, $CDCl_3$), δ (ppm): 8.13 (d, 2H), 7.45–7.37 (m, 4H), 7.35–7.23 (m, 5H), 7.14 (d, 2H), 5.51 (s, 2H). ^{13}C NMR (75 MHz, $CDCl_3$), δ (ppm): 141.33, 137.85, 129.44, 128.12, 127.08, 126.51, 123.69, 121.06, 119.87, 109.56, 47.23. HRMS (MALDI-TOF): *m*/*z* 257.1220 [M^+, calcd 257.1204].

1-(9-Carbazolyl)-1,2,2-triphenylethene (1). To a solution of **5** (1.2 g, 4.66 mmol) in dry THF (40 mL) was added 4.44 mmol of *n*-butyllithium solution (2.5 M in hexane) at 0 ^{o}C under nitrogen. The resulting solution containing **6** was stirred at 0 ^{o}C and 4.44 mmol of benzophenone was then added. The reaction mixture was allowed to warm to room temperature and stirred for another 6 h. The reaction was quenched by adding an aqueous solution of ammonium chloride. The organic layer was extracted with DCM three times. The organic layers were combined, washed with water and dried over anhydrous magnesium sulfate. After solvent evaporation, the crude alcohol (containing excess diphenylmethane) was dissolved in about 50 mL of toluene in a 100 mL two-necked round bottom flask equipped with a condenser. A catalytic amount of *p*-toluenesulphonic acid (TsOH) was then added and the mixture was heated to reflux. After cooled to room temperature, the organic layer was washed with 25 mL of 10% aqueous sodium bicarbonate solution twice and dried over anhydrous magnesium sulfate. After solvent evaporation, the crude product was purified by a silica gel column chromatography using hexane/DCM (4:1 v/v) as eluent. White solid; yield 40.0% (0.75 g). ^{1}H NMR (300 MHz, $CDCl_3$), δ (ppm): 7.98 (d, 2H), 7.27–7.22 (m, 10H), 7.17–7.03 (m, 3H), 7.02–7.01 (m, 3H), 6.91–6.86 (m, 5H). ^{13}C NMR (75 MHz, $CDCl_3$), δ (ppm): 142.27, 142.23, 142.12, 141.01, 138.30, 132.66, 132.20, 130.54, 129.33, 128.91, 128.76, 128.56, 128.37, 128.17, 128.12, 126.29, 124.06, 120.63, 120.29, 111.52. HRMS (MALDI-TOF): *m*/*z* 421.1860 [M^+, calcd 421.1830].

(9-Hexyl-3-carbazolyl)(phenyl)methanone (8a). 9-Hexyl-carbazole was first prepared from carbazole (**4**, 5 g, 29.9 mmol), 1-bromohexane (4.11 g, 24.9 mmol) and tetrabutylammonium bromide (0.80 g, 2.5 mmol) in 50 wt% of aqueous KOH solution (40 mL) and benzene (40 mL). The procedures were similar to those for the synthesis of **5**. Viscous colourless liquid; yield 90.0% (5.66 g). ^{1}H NMR (300 MHz, $CDCl_3$), δ (ppm): 8.10 (d, 2H), 7.46–7.38 (m, 4H), 7.22 (t, 2H), 4.28 (t, 2H), 1.90–1.80 (m, 2H), 1.50–1.24 (m. 6H), 0.86 (t, 3H). ^{13}C NMR (75 MHz, $CDCl_3$), δ (ppm): 141.08, 126.22, 123.46, 121.00, 119.33, 109.31, 43.74, 32.27, 29.61, 27.66, 23.23, 14.71. HRMS (MALDI-TOF): *m*/*z* 251.1683 [M^+, calcd 251.1674].

Into another 100 mL one-necked round bottom flask were added 9-hexyl-carbazole (2 g, 7.96 mmol), benzoyl chloride (**7**, 1.12 g, 7.96 mmol), aluminium chloride (1.11 g, 8.35 mmol) and DCM (40 mL). The reaction mixture was stirred overnight. Large amount of cold water was added to quench the reaction and the reaction mixture was then extracted with DCM. The organic layer was washed with water and dried over magnesium sulfate. After filtration and solvent evaporation, the crude product was purified by silica-gel column chromatography using hexane/DCM (3:2 v/v) as eluent. White solid; yield 84.2% (2.38 g). ^{1}H NMR (300 MHz, $CDCl_3$), δ (ppm): 8.60 (s, 1H), 8.10 (d, 1H), 8.04 (d, 1H), 7.84 (d, 2H), 7.60–7.43 (m, 6H), 7.26 (t, 1H), 4.33 (t, 2H), 1.94–1.84 (m, 2H), 1.42–1.23 (m, 6H), 0.87 (t, 3H). ^{13}C NMR (75 MHz, $CDCl_3$), δ (ppm): 197.30, 143.70, 141.78, 139.71, 132.31, 130.57, 129.09, 128.84, 127.08, 124.72, 123.77, 123.08, 121.38, 120.57, 109.89, 108.94, 44.03, 32.20, 29.59, 27.60, 23.20, 14.68. HRMS (MALDI-TOF): *m*/*z* 355.1933 [M^+, calcd 355.1936].

[4-(Diphenylamino)phenyl](phenyl)methanone (8b). Compound **8b** was prepared from triphenylamine (2 g, 8.15 mmol), benzoyl chloride (1.15 g, 8.15 mmol) and aluminium chloride (1.14 g, 8.55 mmol) in DCM (40 mL). The procedures were similar to those for the synthesis of **8a**. Green solid; yield 80.1% (2.28 g). ^{1}H NMR (300 MHz, $CDCl_3$), δ (ppm): 7.77 (d, 2H), 7.71 (d, 2H), 7.55 (t, 1H), 7.46 (t, 2H), 7.33 (t, 4H), 7.19–7.12 (m, 6H), 7.03 (t, 2H). ^{13}C NMR (75 MHz, $CDCl_3$), δ (ppm): 195.91, 152.60, 147.17, 139.14, 132.65, 132.38, 130.33, 130.29, 130.20, 128.80, 126.67, 125.32, 120.20. HRMS (MALDI-TOF): *m*/*z* 349.1465 [M^+, calcd 349.1467].

1-(9-Hexyl-3-carbazolyl)-1,2,2-triphenylethene (2). To a solution of diphenylmethane (0.50 g, 2.95 mmol) in dry THF (30 mL) was added 2.81 mmol of *n*-butyllithium solution (2.5 M in hexane) at 0 ^{o}C under nitrogen. The resulting solution containing diphenylmethyllithium was stirred at 0 ^{o}C and 2.81 mmol of **8a** was then added. The procedures were similar to those for the synthesis of **1**. White solid; yield 42.9% (0.61 g). ^{1}H NMR (300 MHz, $CDCl_3$), δ (ppm): 7.87 (d, 1H), 7.75 (s, 1H), 7.40 (d, 1H), 7.35 (d, 1H), 7.17–7.02 (m, 18H), 4.21 (t, 2H), 1.85–1.82 (m, 2H), 1.38–1.29 (m, 6H), 0.88 (t, 3H). ^{13}C NMR (75 MHz, $CDCl_3$), δ (ppm): 145.20, 144.98, 142.39, 141.28, 140.62, 139.91, 135.12, 132.27, 132.17, 132.16, 130.28, 129.19, 128.81, 128.29, 128.23, 126.96, 126.81, 126.74, 126.52, 126.06, 124.01, 123.56, 122.97, 120.98, 119.31, 109.30, 108.37, 43.79, 32.22, 29.60, 27.65, 23.24, 14.70. HRMS (MALDI-TOF): *m*/*z* 505.3439 [M^+, calcd 505.2770].

1-[(4-Diphenylamino)phenyl]-1,2,2-triphenylethene (3). To a solution of diphenylmethane (0.45 g, 2.70 mmol) in dry THF (40 mL) was added 2.58 mmol of *n*-butyllithium solution (2.5 M in hexane) at 0 ^{o}C under nitrogen. The resulting solution containing diphenylmethyllithium was stirred at 0 ^{o}C and 2.58 mmol of **8b** was then added. The procedures were similar to those for the synthesis of **1**. White solid; yield 38.8% (0.50 g). ^{1}H NMR (300 MHz, $CDCl_3$), δ (ppm): 7.25–7.21 (m, 4H), 7.19–7.02 (m, 21H), 6.85 (d, 2H), 6.79 (d, 2H). ^{13}C NMR (75 MHz, $CDCl_3$), δ (ppm): 148.28, 146.65, 144.73, 144.47, 144.27, 141.38, 141.16, 138.60, 132.84, 132.06, 129.80, 129.20, 128.82, 128.28, 127.10, 127.01, 124.90, 123.47, 123.35. HRMS (MALDI-TOF): *m*/*z* 499.2428 [M^+, calcd 499.2300].

Acknowledgements

This work was partially supported by the National Basic Research Program of China (973 Program; 2013CB834701), the Research Grants Council of Hong Kong (HKUST2/CRF/10 and N_HKUST620/11), the Innovation and Technology Commission (ITCPD/17-9) and the University Grants Committee of Hong Kong (AoE/P-03/08 and T23-713/11-1). B.Z.T. thanks the support of the Guangdong Innovative Research Team Program (201101C0105067115).

Notes and references

[a] Department of Chemistry, Institute for Advanced Study, Institute of Molecular Functional Materials, Division of Life Science, Division of Biomedical Engineering and State Key Laboratory of Molecular Neuroscience, The Hong Kong University of Science & Technology (HKUST), Clear Water Bay, Kowloon, Hong Kong, China. E-mail: tangbenz@ust.hk
[b] State Key Laboratory of Luminescent Materials and Devices, South China University of Technology (SCUT), Guangzhou 510640, China.
[c] Centre for Display Research, The Hong Kong University of Science & Technology, Clear Water Bay, Kowloon, Hong Kong, China.
[d] State Key Laboratory of Supermolecular Structure and Materials, Jilin University, Changchun 150012, China.
[e] Guangdong Innovative Research Team, SCUT-HKUST Joint Research Laboratory, South China University of Technology (SCUT), Guangzhou 510640, China.
[f] HKUST-Shenzhen Research Institute, No. 9 Yuexing 1st RD, South Area, Hi-tech Park, Nanshan, Shenzhen 518057, China.

† Electronic Supplementary Information (ESI) available: Crystal data of **1**–**3** and supplementary figures. CCDC reference numbers CCDC 970451–970453. See DOI: 10.1039/b000000x/

1 (a) C. W. Tang, S. A. VanSlyke, *Appl. Phys. Lett.*, 1987, **51**, 913; (b) C. W. Tang, S. A. VanSlyke, C. H. Chen, *J. Appl. Phys.*, 1989, **65**, 3610.
2 (a) J. B. Birks, *Photophysics of Aromatic Molecules*, Wiley, London, UK, 1970; (b) I. Capek, *Adv. Colloid Interf. Sci.*, 2002, **97**, 91; (c) S. W. Thomas III, G. D. Joly, T. M. Swager, *Chem. Rev.*, 2007, **107**, 1339; (d) F. Mancin, P. Scrimin, P. Tecilla, U. Tonellato, *Coord. Chem. Rev.*, 2009, **253**, 2150.
3 (a) J. Luo, Z. Xie, J. W. Y. Lam, L. Cheng, H. Chen, C. Qiu, H. S. Kwok, X. Zhan, Y. Liu, D. Zhu, B. Z. Tang, *Chem. Commun.*, 2001, 1740; (b) B. Z. Tang, X. Zhan, G. Yu, P. P. S. Lee, Y. Liu, D. Zhu, *J. Mater. Chem.*, 2001, **11**, 2974; (c) Y. Hong, J. W. Y. Lam, B. Z. Tang, *Chem. Soc. Rev.*, 2011, **40**, 5361; (d) Z. Zhao, J. W. Y. Lam, B. Z. Tang, *Curr. Org. Chem.*, 2010, **14**, 2109; (e) J. Liu, J. W. Y. Lam, B. Z. Tang, *J. Inorg. Organomet. Polym. Mater.*, 2009, **19**, 249; (f) Y. Hong, J. W. Y. Lam, B. Z. Tang, *Chem. Commun.*, 2009, 4332.
4 (a) M. Levitus, K. Schmieder, H. Ricks, K. D. Shimizu, U. H. F. Bunz, M. A. Garcia-Garibay, *J. Am. Chem. Soc.*, 2001, **123**, 4259; (b) B.-K. An, S.-K. Kwon, S.-D. Jung, S. Y. Park, *J. Am. Chem. Soc.*, 2002, **124**, 14410; (c) C. Belton, D. F. O'Brien, W. J. Blau, A. J. Cadby, P. A. Lane, D. D. C. Bradley, H. J. Byrne, R. Stockmann, H.-H. Hörhold, *Appl. Phys. Lett.*, 2001, **78**, 1059; (d) L. Antolini, E. Tedesco, G. Barbarella, L. Favaretto, G. Sotgiu, M. Zambianchi, D. Casarini, G. Gigli, R. Cingolani, *J. Am. Chem. Soc.*, 2000, **122**, 9006; (e) R. Deans, J. Kim, M. R. Machacek, T. M. Swager, *J. Am. Chem. Soc.*, 2000, **122**, 8565.
5 (a) K. Mullen, U. Scherf, *Organic Light-Emitting Devices. Synthesis, Properties and Applications*, Wiley: Weinheim, Germany, 2006; (b) J. Roncali, P. Leriche, A. Cravino, *Adv. Mater.*, 2007, **19**, 2045; (c) B. Liu, T. T. T. Dan, G. C. Bazan, *Adv. Funct. Mater.*, 2007, **17**, 2432; (d) S. H. Yang, C. S. Hsu, *J. Polym. Sci. Part A: Polym. Chem.*, 2008, **46**, 7173.
6 Y. Dong, J. W. Y. Lam, A. Qin, J. Liu, Z. Li, B. Z. Tang, *Appl. Phys. Lett.*, 2007, **91**, 011111.
7 Z. Zhao, C. Y. K. Chan, S. Chen, C. Deng, J. W. Y. Lam, C. K. W. Jim, Y. Hong, P. Lu, Z. Chang, X. Chen, P. Lu, H. S. Kwok, H. Qiu, B. Z. Tang, *J. Mater. Chem.*, 2012, **22**, 4527.
8 Y. Liu, S. Chen, J. W. Y. Lam, P. Lu, R. T. K. Kwok, F. Mahtab, H. S. Kwok, B. Z. Tang, *Chem. Mater.*, 2011, **23**, 2536.
9 Y. Sagara and T. Kato, *Nat. Chem.*, 2009, **1**, 605.
10 (a) I. B. Berlman, *Handbook of Fluorescence Spectra of Aromatic Molecules*, Academic Press, New York and London, 1971. (b) W. Yuan, P. Lu, S. Chen, J. W. Y. Lam, Z. Wang, Y. Liu, H. S. Kwok, Y. Ma, B. Z. Tang, *Adv. Mater.*, 2010, **22**, 2159.
11 (a) H. Tian, J. A. Gan, K. C. Chen, J. He, Q. L. Song, X. Y. Hou, *J. Mater. Chem.*, 2002, **12**, 1262; (b) T. Mutai, H. Satou, K. Araki, *Nat. Mater.*, 2005, **4**, 685; (c) G. Y. Jiang, S. Wang, W. Yuan, L. Jiang, Y. L. Song, H. Tian, D. B. Zhu, *Chem. Mater.*, 2006, **18**, 235.

 This journal is © The Royal Society of Chemistry 2012